A Capacitive MEMS Viscometric Sensor for Affinity Detection of Glucose

Xian Huang, Siqi Li, Jerome Schultz, Qian Wang, and Qiao Lin

***Abstract*—This paper presents a capacitively based microelectromechanical systems affinity sensor for continuous glucose monitoring (CGM) applications. This sensor consists of a vibrating Parylene diaphragm, which is remotely driven by a magnetic field and situated inside a microchamber. A solution of poly(acrylamide-ran-3-acrylamidophenylboronic acid) (PAA-*ran*-PAAPBA), a biocompatible glucose-sensitive polymer, fills the microchamber, which is separated from its surroundings by a semipermeable membrane. Glucose permeates through the membrane and binds reversibly to the phenylboronic acid moiety of the polymer. This results in a viscosity change of the sensing solution, causing a detectable change in the Parylene diaphragm vibration which can be measured capacitively. Experimental results demonstrate that the device is capable of detecting glucose at physiologically relevant concentrations ranging from 30 to 360 mg/dL. The response time of the sensor to glucose concentration changes is approximately 1.5 min, which can be further improved with optimized device designs. Excellent reversibility and stability are observed in sensor responses, as highly desired for long-term CGM. [2009-0171]**

***Index Terms*—Affinity binding, biocompatibility, biosensor, continuous glucose monitoring (CGM), diabetes, viscometry.**

I. Introduction

DIABETES mellitus is a metabolic disease characterized by persistent hyperglycemia (high blood sugar levels). Close monitoring of daily blood sugar levels reduces the risk of diabetes-related complications by allowing timely identification and correction of hyperglycemia as well as hypoglycemia (low blood sugar levels), a condition that typically results from excessive insulin uptake or inadequate glucose intake. This can be most effectively achieved by continuous glucose monitoring (CGM), which involves constantly repetitive measurements of physiological glucose levels.

Currently, subcutaneously implanted enzymatic electrochemical detection is the prevailing CGM technique and is the basis for several commercially available devices, such as Medtronic MiniMed Paradigm [1], Freestyle Navigator [2], and DexCom Seven Plus [3]. Electrochemical methods are capable of sensitive and specific glucose detection but suffer from some significant drawbacks. The irreversible consumption of glucose in electrochemical detection induces a potential change in the equilibrium glucose concentration in the tissue and thus affects the actual measured glucose level. In addition, the rate of glucose consumption is diffusion limited. Any changes in diffusion layers due to biofouling (e.g., by protein adsorption, cell deposition, and capsule formation) on the sensor surface affect the diffusion rate and, thus, the device sensitivity. Moreover, drift from hydrogen peroxide production and interference from electrode-active chemicals may cause erosion of the sensor electrodes and deactivation of functional enzymes, compromising the device accuracy, reliability, and longevity [4]. As a result, electrochemical CGM sensors generally exhibit large drifts over time and require frequent calibration by finger pricks (typically at least once every 12 h) [1], [3]. This lack of reliability has been severely hindering CGM applications to practical diabetes management.

To overcome the drawbacks of electrochemical detection, alternative subcutaneously based glucose sensing techniques have been under active investigation. In particular, methods that use equilibrium affinity binding of glucose have shown great promise [5]–[8]. These methods, in which glucose is not consumed, do not carry the risk of interfering with the local glucose concentration in the tissue or generating erosive reaction products. More importantly, affinity sensing is considerably more stable and low drift in the face of biofouling, as the deposition of biological material on the implanted sensor surface results only in an increased equilibration time without any changes in measurement accuracy. A widely used affinity sensing technique is based on concanavalin A (Con A), whose specific binding to glucose can be detected via methods such as fluorescence [5], [6] and viscosity [7]. Unfortunately, Con A is immunogenic and cytotoxic [9] and degrades with time [10]. Alternatively, affinity sensing systems utilizing synthetic glucose-binding polymers have the potential to address these issues [11]. In particular, polymers containing boronic acid groups bind to glucose specifically at physiological pH values [12] and have been developed to enable a variety of glucose detection methods such as fluorescence [13], volume change [14], and conductometry [15]. Recently, we developed a novel boronic-acid-based affinity sensing system that uses the polymer poly(acrylamide-*ran*-3-acrylamidophenylboronic acid) (PAA-*ran*-PAAPBA) [16], [17]. In the system, glucose reversibly forms strong ester bonds with the phenylboronic acid moiety on the backbone of PAA-*ran*-PAAPBA, resulting in

Manuscript received July 8, 2009; revised September 22, 2009. First published November 13, 2009; current version published December 1, 2009. This work was supported in part by the National Science Foundation under Grant ECCS-0702101 and in part by the Columbia Diabetes and Endocrinology Research Center under NIH Grant DK63068-05. The work of X. Huang was supported in part by a national scholarship program from the China Scholarship Council. Subject Editor A. J. Ricco.

X. Huang and Q. Lin are with the Department of Mechanical Engineering, Columbia University, New York, NY 10027 USA (e-mail: qlin@columbia.edu).

S. Li and Q. Wang are with the Department of Chemistry and Biochemistry and Nanocenter, University of South Carolina, Columbia, SC 29208 USA.

J. Schultz is with the Department of Bioengineering, University of California, Riverside, CA 92521 USA.

Color versions of one or more of the figures in this paper are available online at http://ieeexplore.ieee.org.

Digital Object Identifier 10.1109/JMEMS.2009.2034869

1057-7157/$26.00 © 2009 IEEE

Authorized licensed use limited to: Columbia University. Downloaded on January 19, 2010 at 13:06 from IEEE Xplore. Restrictions apply.

cross-linking of the polymer and an increase in the viscosity of the solution.

Microelectromechanical systems (MEMS) technology holds the potential to allow integrated implantable sensors for metabolic monitoring, whose miniature sizes would lead to improved measurement time response and minimized invasiveness. MEMS and related technologies have been applied to glucose sensors that are based on electrochemical [18], [19], impedimetric [20], eletrophoretic [21], thermal [16], [22], [23], optical [24], and colorimetric [25] detection methods. MEMS glucose sensors have also exploited microdialysis [26] and glucose-induced hydrogel swelling [14]. We have previously reported a MEMS affinity glucose sensor in which a vibrational cantilever was used for viscometric measurements of glucose binding with Con A [7]. Recently, we presented an improved device in which Con A, which is not biocompatible, was replaced with a nontoxic synthetic polymer [27]. These devices demonstrated the feasibility of viscosity-based affinity glucose sensing but required the use of an optical lever setup to measure the cantilever deflection, which is not compatible with subcutaneously implanted operation.

This paper presents a major improvement to our previously reported devices [7], [27] by integration of capacitive detection within a MEMS affinity glucose sensor. The device consists of a microchamber that is equipped with a semipermeable membrane and filled with a solution of a glucose-specific synthetic polymer. Glucose permeates through the semipermeable membrane and binds reversibly to the polymer, causing cross-linking of the polymer and changing the viscosity of the solution. The viscosity change causes variations in the viscous damping on the magnetically driven vibration of a flexible diaphragm, whose deflection results in changes of the capacitance between two electrodes, one of which is embedded in the diaphragm. Thus, the capacitance change can be measured to detect the damped diaphragm vibration and further determine the interstitial fluid glucose concentration.

II. Principle and Design

As shown in Fig. 1, the MEMS affinity glucose sensor is based on a freestanding Parylene diaphragm that is situated inside a microchamber. The microchamber is filled with the solution of a biocompatible polymer that binds specifically and reversibly with glucose, and is equipped with a cellulose acetate semipermeable membrane, which allows glucose to permeate into and out of the chamber while keeping the glucose-sensitive polymer from escaping. The diaphragm is embedded with a moving gold electrode, which forms a capacitor with a fixed gold electrode on the substrate below. Separating the electrodes is a sealed air gap. A set of Permalloy thin-film strips is also integrated on the diaphragm. The Permalloy strips and moving electrode are passivated to avoid direct contact with the polymer solution. The dimensions of these components are shown in Fig. 1.

The MEMS device utilizes poly(acrylamide-ran-3-acrylamidophenylboronic acid) (PAA-*ran*-PAAPBA), which is a biocompatible polymer and recognizes glucose by specific affinity binding [16], [17]. PAA-*ran*-PAAPBA is

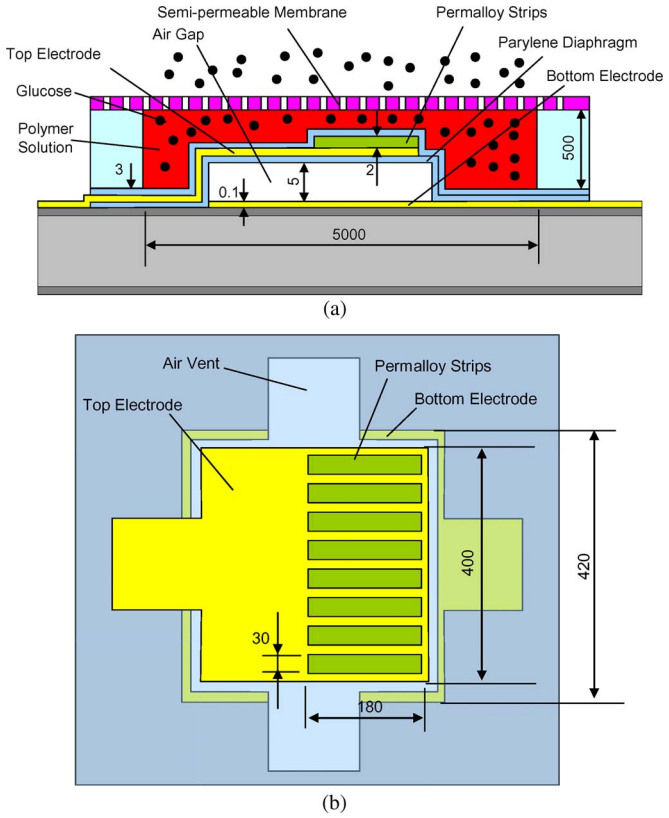

Fig. 1. Schematic of the MEMS capacitive glucose sensor: (a) Side view of the capacitive glucose sensor and (b) top view of the capacitive glucose sensor (dimensions are given in micrometers).

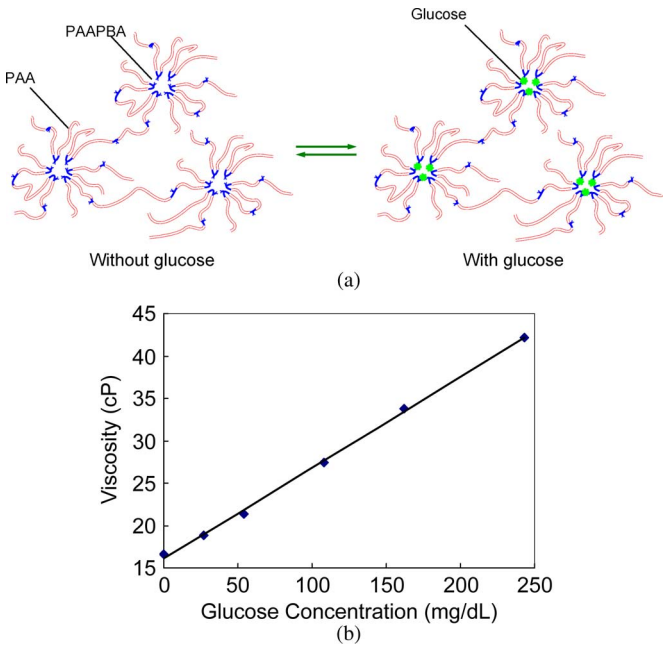

Fig. 2. Poly(acrylamide-ran-3-acrylamidophenylboronic acid) (PAA-ran-PAAPBA), a biocompatible glucose-specific polymer. (a) Polymer composition and mechanism of interaction with glucose. (b) Glucose-induced viscosity change of a 5% PAA-*ran*-PAAPBA solution in PBS buffer (pH 7.4).

an amphiphilic copolymer containing two components: poly(3-acrylamidophenylboronic acid) (PAAPBA) and polyacrylamide (PAA) [Fig. 2(a)]. PAAPBA is a hydrophobic glucose-sensitive component, while PAA is hydrophilic and

Authorized licensed use limited to: Columbia University. Downloaded on January 19, 2010 at 13:06 from IEEE Xplore. Restrictions apply.

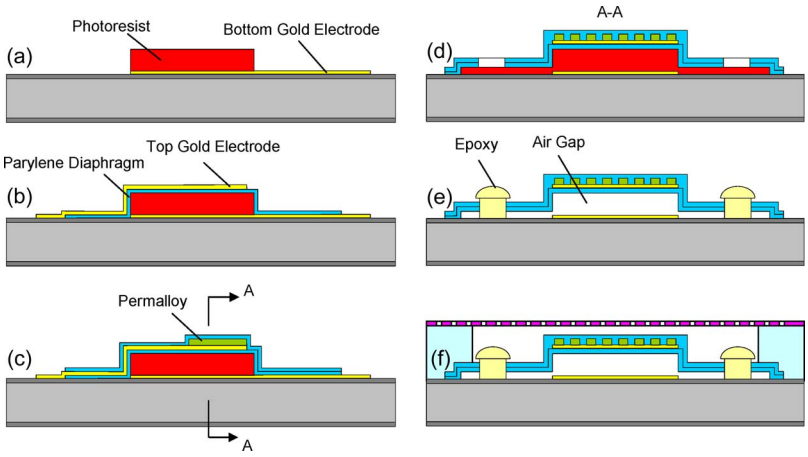

Fig. 3. Fabrication process. (a) Bottom gold electrode deposition and sacrificial layer patterning. (b) Parylene deposition and top gold electrode deposition. (c) Permalloy electroplating and additional Parylene layer deposition. (d) Photoresist etching hole patterning. (e) Sacrificial layer removal and diaphragm releasing. (f) Membrane bonding and device packaging.

primarily serves to improve the overall water solubility of the polymer. When added to an aqueous solution of PAA-*ran*-PAAPBA, glucose binds reversibly to the phenylboronic acid moieties in the PAAPBA segment to form strong cyclic boronate ester bonds, resulting in an increase in the viscosity of the solution [Fig. 2(b)].

When glucose permeates through the semipermeable membrane, it interacts with PAA-*ran*-PAAPBA to result in a reversible viscosity change, which is detected via vibration measurements. Specifically, an externally applied time-varying magnetic field acts upon the Permalloy strips, which are magnetized along their length by a permanent magnet. This results in a time-varying moment in the Permalloy, directed in the in-plane direction perpendicular to the strip length. Under the action of the moment, the diaphragm vibrates, whose deflection is detected from the capacitance change between the electrodes. As the viscous damping on the vibration directly depends on viscosity, the measured capacitance change can be used to determine the viscosity change and, hence, the glucose concentration.

III. Fabrication Process

As shown in Fig. 3, the device fabrication process began with the deposition and patterning of chrome (5 nm) and gold (100 nm) to form the fixed electrode $(420 \times 420 \times 0.1\ \mu\text{m}^3)$ on the thermally grown SiO_2 layer on a silicon wafer. A sacrificial photoresist layer (5 μm) was then spin coated and patterned to define the electrode air gap [Fig. 3(a)], followed by the deposition of a Parylene layer (3 μm). A second layer of chrome (5 nm) and of gold (100 nm) were next deposited for the moving electrode $(400 \times 400 \times 0.1\ \mu\text{m}^3)$ and Permalloy seed layer [Fig. 3(b)]. Subsequently, with the Permalloy strips defined by a photoresist mold (5 μm), Permalloy (2 μm) was electroplated. This was followed by the removal of the photoresist mold, patterning of the moving gold electrode, and deposition of an additional Parylene layer (3 μm) for passivation [Fig. 3(c)]. Two etching holes $(500 \times 500\ \mu\text{m}^2)$ were opened through the two Parylene layers by oxygen plasma to expose the sacrificial photoresist layer [Fig. 3(d)], which was subsequently removed by acetone (80 °C) to release the diaphragm. These two etching holes were then sealed by epoxy (Devcon) [Fig. 3(e)]. After wafer dicing and wire bonding, a chip was bonded to a polycarbonate sheet (thickness: 500 μm), in which holes of appropriate sizes were drilled to define the microchamber as well as the inlet and outlet (each 10 μL) for polymer solution handling. The polycarbonate was, in turn, bonded to a regenerated cellulose acetate semipermeable membrane (Fisher) with a molecular weight cutoff of 3500 Da and thickness of 20 μm using epoxy [Fig. 3(f)].

IV. Experimental Method

The PAA-*ran*-PAAPBA polymer was synthesized in house by free radical polymerization [16], [17]. To prepare the polymer solution, 284 mg of PAA-*ran*-PAAPBA, with an acrylamide (AA) to 3-acrylamidophenylboronic acid (AAPBA) molar ratio of 20 (or approximately 5% PAAPBA content in the polymer) and a molecule weight of 170 700, was dissolved in 6 mL of phosphate buffer saline (PBS). The PBS buffer (pH 7.4) was prepared from potassium phosphate (20 mM), NaCl (150 mM), and NaN_3 (0.05%). D-(+)-glucose was purchased from Sigma-Aldrich. Glucose stock solution (1 M) was prepared by dissolving glucose (1.8 g) in PBS to 10 mL. A series of glucose solutions (30, 60, 90, 120, 210, and 360 mg/dL) was prepared by further diluting the stock solution with PBS.

All experiments with the MEMS affinity glucose sensor were conducted at 37 °C with closed-loop temperature control to simulate a physiologically relevant glucose monitoring condition and minimize temperature-dependent viscosity changes. During testing, the device's microchamber was filled with an initially glucose-free solution of PAA-*ran*-PAAPBA (PAAPBA content: 5%). To facilitate experimentation, a test cell (volume: 300 μL) was constructed from a polycarbonate sheet directly above the MEMS device [Fig. 4(a)]. A glucose solution at a given concentration was introduced into the test cell, where it was allowed to permeate through the device's semipermeable membrane to interact with PAA-*ran*-PAAPBA in the microchamber. Because the volume of the test cell was 30 times that of the chamber, it was reasonably assumed that

Authorized licensed use limited to: Columbia University. Downloaded on January 19, 2010 at 13:06 from IEEE Xplore. Restrictions apply.

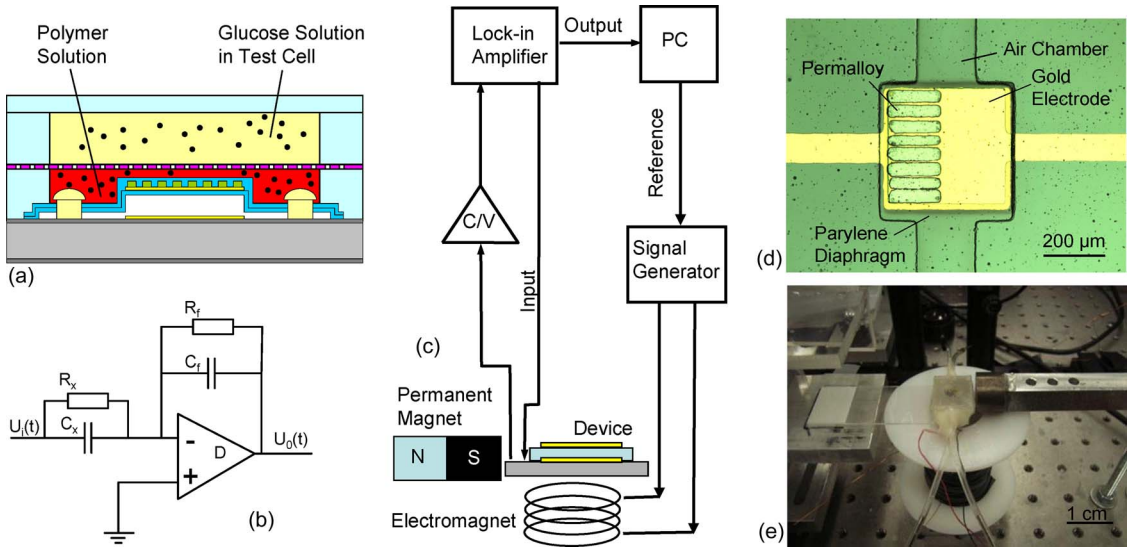

Fig. 4. Experimental setup for characterization of the MEMS affinity glucose sensor. (a) Schematic of the sensor outfitted with a flow cell containing glucose solution. (b) Capacitive measurement circuitry. (c) Experimental setup and images of a MEMS affinity glucose sensor: (d) Before and (e) after packaging and putting into the measurement system.

the glucose concentration inside the microchamber equalized to the given glucose concentration in the test cell when the glucose permeation reached an equilibrium.

The sensor capacitance was measured using a capacitance–voltage transformation circuit [Fig. 4(b)]. Given an input sinusoidal wave U_i (1 $V_{\rm rms}$), the output voltage U_0 had an amplitude that was proportional to the ratio of the sensor capacitance C_x (98 pF in the absence of diaphragm motion) to the standard reference capacitance C_f (330 pF). This output was captured by a lock-in amplifier and acquired by a personal computer. In the experimental setup [Fig. 4(c)], the diaphragm vibration was driven by a home-made solenoid (400 turns of a 250-μm-diameter copper wire on a plastic core), which, under a driving voltage of 10 $V_{\rm pp}$, produced a magnetic field strength of about 950 A/m at 1000 Hz perpendicular to the cantilever surface. A permanent magnet bar with a field strength of approximately 200 kA/m was placed parallel to the Permalloy strips to yield saturated magnetization of the Permalloy. A fabricated, not yet packaged, device is shown in Fig. 4(d), while a packaged device in the experimental setup is shown in Fig. 4(e).

V. Results and Discussion

This section presents and analyzes experimental results from a fabricated MEMS affinity glucose sensor. We first evaluate the device's vibration characteristics at physiologically relevant glucose concentrations under various excitation frequencies and then analyze the observed characteristics with a simplified oscillator model. The temporal course of the diaphragm vibration due to glucose concentration changes is then observed to determine the device's time response and examine its reversibility. Finally, the drift in the device response in glucose measurements over an extended measuring period is investigated to evaluate the device's potential suitability for long-term stable CGM applications.

A. Measured Diaphragm Vibration Characteristics

The dependence of vibration characteristics of the sensor diaphragm on the excitation frequency was first characterized. In the experiment, the glucose concentration was first allowed to be equilibrated at a physiologically relevant value (30, 60, 90, 120, 210, or 360 mg/dL). The diaphragm vibrated under the excitation of a harmonically time-varying magnetic field, which had a frequency-independent amplitude of approximately 110 A/m. The steady-state amplitude and phase of the diaphragm vibration as a function of the excitation frequency were obtained in terms of the output voltage of the capacitive measurement circuit (Fig. 4). As shown in the amplitude frequency response [Fig. 5(a)], the diaphragm vibration exhibited resonance behavior at all glucose concentrations tested. The resonance peaks were relatively broad because of significant damping from the highly viscous polymer solution. As the glucose concentration increased from 30 to 360 mg/dL, the resonance peak decreased consistently by 53 mV (from 542 to 489 mV). This was accompanied by a downward shift of the resonance frequency by 100 Hz (from 1000 to 900 Hz). These observations indicate a significant increase in vibrational damping, which is consistent with the increased viscosity of the polymer solution at higher glucose concentrations.

In addition, from the phase frequency response [Fig. 5(b)], it can be seen that, at a given frequency, there was a significant change in the phase shift between the diaphragm vibration and the magnetic excitation. For example, at 400 Hz, the phase shift decreased from 17.68° at 30 mg/dL to 7.69° at 360 mg/dL, which again agrees with the increased damping at higher glucose concentrations. It is interesting to note that the phase shift curves at the different glucose concentrations intersect at a single frequency of approximately 1200 Hz, at which the phase shift was 91.8°. This is consistent with the behavior of a single-degree-of-freedom damped harmonic oscillator and suggests that the natural frequency of the diaphragm, taking into account the added mass from the polymer solution, was about 1200 Hz.

Authorized licensed use limited to: Columbia University. Downloaded on January 19, 2010 at 13:06 from IEEE Xplore. Restrictions apply.

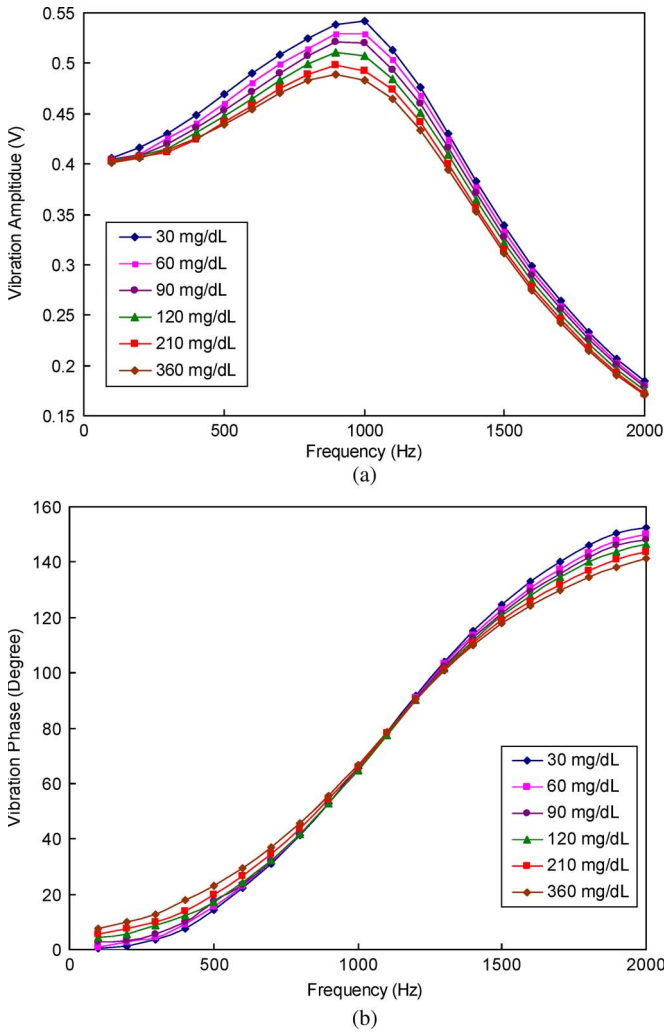

Fig. 5. Frequency-dependent behavior of the harmonically driven vibration of the sensor diaphragm at physiologically relevant glucose concentrations: (a) Amplitude and (b) phase shift.

B. Analysis of Diaphragm Vibration Characteristics With a Simplified Model

The diaphragm vibration is, in general, a complex physical phenomenon involving the intimate coupling of the motion of the continuously deflecting diaphragm and the flow of the viscous polymer solution. Nonetheless, useful insight can be gained into this phenomenon with a simplified analysis, in which we represent the diaphragm as a one-degree-of-freedom (1-DOF) mass-spring-damper system. In this system, the Permalloy strips are collectively represented as a 1-DOF rigid plate that can rotate about a fixed axis under a magnetically applied torque. The diaphragm outside the plate region is assumed to have negligible inertia while applying a linear elastic restoring torque on the plate. The interaction of the plate and diaphragm motion with the polymer solution can be represented as a linear viscous torque. Then, the equation governing the plate rotation θ under a torque $T(t)$ takes the form

$$I\ddot{\theta} + D\dot{\theta} + K\theta = T(t) \tag{1}$$

where I is the plate's moment of inertia, D is the viscous damping coefficient, and K is the diaphragm's spring constant.

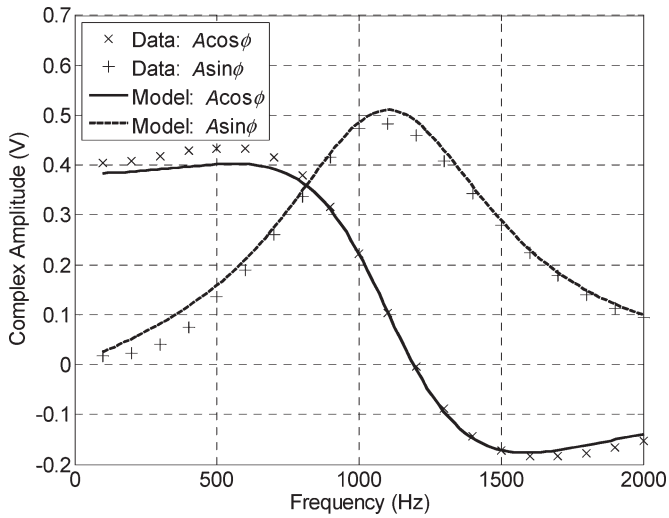

Fig. 6. One-DOF mass-spring-damper model fitted to the experimental data obtained at a glucose concentration of 90 mg/dL. A single set of parameters $\theta_m = 0.38$ V, $f_0 = 1190$ Hz, and $\zeta = 0.39$ allowed the model to fit two sets of data, which are experimentally determined values of the real and imaginary parts of the complex amplitude.

Consider the steady-state motion of the Permalloy plate under a harmonic magnetic excitation, i.e., $T(t) = T_m e^{i\omega t}$, at frequency $f = \omega/2\pi$. Equation (1) can be reformulated into a form

$$\ddot{\theta} + 2\zeta\omega_0\dot{\theta} + \omega_0^2\theta = \theta_m e^{i\omega t} \tag{2}$$

where $\omega_0 = 2\pi f_0 = (K/I)^{1/2}$ is the natural frequency and $\zeta = (1/2)D/(IK)^{1/2}$ is the dimensionless damping ratio. In addition, $\theta_m = T_m/I$ is the plate rotation at zero excitation frequency.

The steady-state solution to (2) is of the form $\theta = Ae^{-i\phi}e^{i\omega t}$, where $Ae^{-i\phi}$ is the complex amplitude with the amplitude (A) and phase shift (ϕ) of the plate rotation. By defining $p = f/f_0$, these quantities are given by

$$\begin{aligned} A_x &= A\cos\phi = \theta_m(1-p^2)/\left[(1-p^2)^2 + 4\zeta^2p^2\right] \\ A_y &= A\sin\phi = \theta_m(2\zeta p)/\left[(1-p^2)^2 + 4\zeta^2p^2\right]. \end{aligned} \tag{3}$$

Equation (3) can now be fitted to the experimental data, recognizing that the diaphragm rotation is proportional to the sensor output. For example, the case of the glucose concentration at 90 mg/dL is shown in Fig. 6. Here, it is important to note that, to obtain consistent results, it is not appropriate to fit A_x or A_y (or, equivalently, A or ϕ) independently to the data. Instead, it is necessary to fit a vector-valued function $\{A_x, A_y\}$ as a function of f as given in (3) to the experimental data, yielding consistent estimates of the parameters θ_m, f_0, and ζ. For the case shown in Fig. 6, a least square fit yields the estimates $f_0 = 1190$ Hz and $\theta_m = 0.38$ V, with $\zeta = 0.39$ (based on the experimental data, θ_m has the dimension of a voltage). As can be seen from the figure, the model agrees with the experimental data well, considering that the fitting involves a vector-valued function, i.e., the model must fit two sets of experimental data with a single set of parameter estimates.

Authorized licensed use limited to: Columbia University. Downloaded on January 19, 2010 at 13:06 from IEEE Xplore. Restrictions apply.

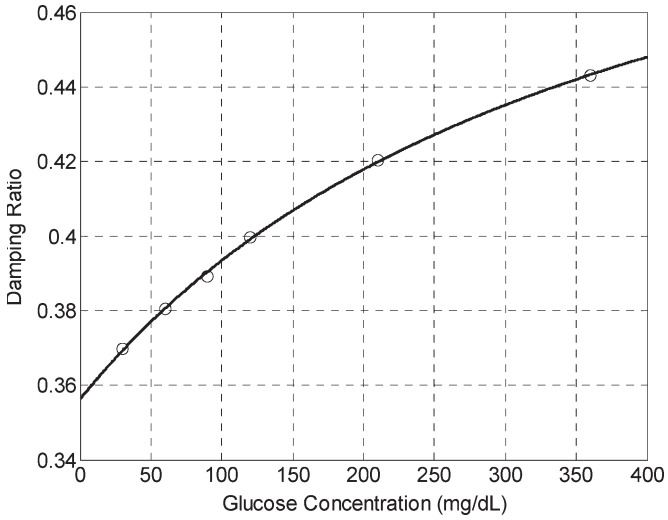

Fig. 7. Damping ratio obtained by fitting the 1-DOF mass-spring-damper model to the experimental data at varying glucose concentrations.

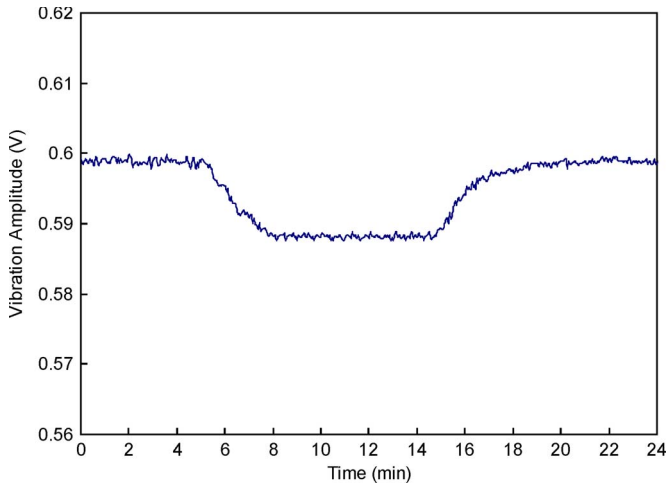

Fig. 8. Time course of the diaphragm vibration amplitude at 1000 Hz as the sensor responded to glucose concentration changes from 90 to 120 mg/dL, which was then reversed to 90 mg/dL.

The model given by (3) can also be fitted to the experimental data obtained at other glucose concentrations as shown in Fig. 7. The value of θ_m is consistently estimated to be almost constant at 0.38 V, with variations less than 0.9% as the glucose concentration varies from 30 to 360 mg/dL. In addition, the estimated natural frequency f_m changes only by 0.6%, suggesting that inertial contributions of viscous effects are insignificant. On the other hand, as shown in Fig. 7, the damping ratio estimated from the fits increases steadily by 20% as the glucose concentration varies from 30 to 360 mg/dL. This is consistent with the increased viscosity of the polymer solution at elevated glucose concentrations.

C. Time-Resolved Measurements of Sensor Response to Glucose Concentration Changes

Having systematically characterized the diaphragm vibration characteristics, we next performed time-resolved measurements of the diaphragm vibration in response to glucose concentration changes, which allowed us to assess the time response, reversibility, and drift in the sensor response.

To characterize the device time response, the glucose concentration was initially allowed to be equilibrated at 90 mg/dL in the test cell and sensor chamber. Next, the solution in the test cell was replaced with another glucose solution at 120 mg/dL. When the glucose concentration inside the sensor chamber had equilibrated to 120 mg/dL, the reverse process was initiated, in which the test cell was refilled with a 90-mg/dL glucose concentration. Some of the polymer-bound glucose molecules dissociated and permeated out of the semipermeable membrane, allowing the glucose concentration inside the sensor chamber to equilibrate to 90 mg/dL. The process of solution refilling of the test cell lasted about 10 s, which was sufficiently fast when compared with the glucose concentration equilibration. During the equilibration processes, the harmonic vibration of the diaphragm, at a fixed frequency of 1000 Hz, was measured as a function of time. The use of a fixed frequency allowed us to use a much larger excitation magnetic field amplitude (250 A/m) than that used above (110 A/m) when the frequency was varied, which was limited by the frequency dependence of the magnetic field generated by the voltage-controlled solenoid.

From the experimental data (Fig. 8), it can be seen that, as the glucose concentration varied from 90 to 120 mg/dL, the diaphragm vibration amplitude decreased with time, corresponding to the increased damping on the diaphragm vibration due to glucose binding-induced viscosity increase. The vibration amplitude finally saturated to a constant level, reflecting that the process of glucose permeation and binding had reached a dynamic equilibrium. The time constant of this process was determined to be approximately 1.5 min. In the reverse process where the glucose concentration in the test cell was decreased from 120 to 90 mg/dL, the vibration amplitude increased with time due to reduced viscous damping from the polymer solution. The time constant for the reverse process was approximately 1.7 min. The longer reverse time constant could be due to the smaller diffusivity of glucose molecules in the initially more viscous polymer solution and needs to be investigated in future work. Note that these time constants compare favorably with response times of commercially available systems that range from 5 to 15 min [1]–[3], and can be further reduced by shortening the distance between the semipermeable membrane and the diaphragm.

It is interesting to examine the measured time constants with respect to estimates based on consideration of glucose diffusion into the sensor. The timescale for glucose molecules to diffuse through the semipermeable membrane and the device microchamber can be estimated to be $t_{\rm diff} \sim (d_m^2/\lambda + d_f^2)/D_g$, where D_g is the glucose diffusivity in the PAA-*ran*-PAAPBA polymer solution, d_m and λ are, respectively, the thickness and porosity of the semipermeable membrane, and d_f is the effective height of the microchamber accounting for the deflection of the membrane caused by sample loading in the test cell. We estimate that D_g is on the order of 3×10^{-11} m/s^2 according to glucose diffusivity in water $(7.1 \times 10^{-10}$ m/s$^2)$ scaled by the ratio of water viscosity to the viscosity of the PAA-*ran*-PAAPBA solution at relevant glucose concentrations. The other

Authorized licensed use limited to: Columbia University. Downloaded on January 19, 2010 at 13:06 from IEEE Xplore. Restrictions apply.

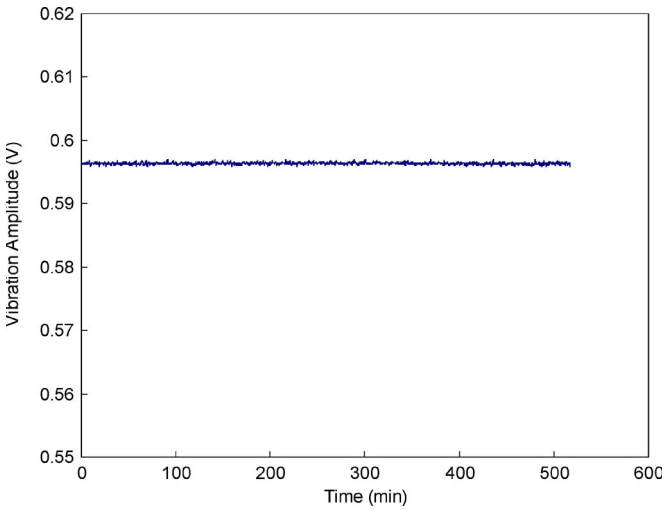

Fig. 9. Diaphragm vibration amplitude at 1000 Hz over an extended time duration as the glucose concentration was held constant at 90 mg/dL.

parameters are estimated to be $d_m \approx 20\ \mu$m, $\lambda \approx 0.6$ [28], and $d_f \approx 100\ \mu$m. Thus, the diffusion timescale is estimated to be 6 min. This provides a theoretical estimate of the time required by the device to respond to glucose concentration changes, which may be considered to have the same order of magnitude as the experimentally determined glucose response time constants. Numerical simulations of the glucose diffusion process can be conducted in future work to more accurately calculate the device's glucose response time.

Experiments have also allowed us to assess the reversibility of the device response, which can be obtained by comparing differences in sensor output between two separated measurements at the same glucose concentration. For example, as shown in Fig. 8, the sensor output at 1000 Hz varied from 0.598 (averaged over the period [0, 5] min) to 0.588 V (averaged over [9, 14] min) as the glucose concentration varied from 90 to 120 mg/dL. The sensor output then returned to 0.598 V (averaged over [19, 24] min) when the glucose concentration was reversed to 90 mg/dL. The difference between the average sensor outputs over the two periods with the glucose concentration at 90 mg/dL was only about 0.3 mV or 60 ppm. Thus, there is excellent reversibility in our sensor with respect to glucose concentration variations.

In general, the measurement accuracy of the sensor is primarily determined by three factors. That is, in addition to reversibility considerations mentioned earlier, the device accuracy is also limited by the repeatability of the sensor output from multiple measurements at a certain glucose concentration and the noise in the measurement as the glucose concentration is held constant. In terms of repeatability, for example, we performed multiple measurements of glucose samples at 90 mg/dL at 1000 Hz, which resulted in the sensor output differing by only about 90 ppm. On the other hand, the accuracy was more significantly influenced by the measurement noise, which can be observed in Fig. 8 (and also in Fig. 9). This noise could be attributed to randomly present tiny air bubbles in the polymer solution that influenced the diaphragm vibration, as well as small temperature fluctuations in the chamber due to limitations in temperature control. The noise, characterized by standard deviations from Fig. 8, was about 0.32 mV or 3% of the sensor output change (10.7 mV) as the glucose concentration was varied from 90 to 120 mg/dL. This translates into a glucose measurement resolution of about 1.8 mg/dL at 90 mg/dL, which is considered to be excellent in the context of practical applications, and can be further improved by improved sensor designs.

Finally, we investigated the drift of the device output by exposing it to constant glucose concentrations over long periods. For example, the harmonic vibration amplitude at 1000 Hz as the glucose concentration was held constant at 90 mg/dL is shown in Fig. 9. It can be seen that the sensor output was steady at 0.596 V over a period of about 9 h, with a drift rate of less than 10 μV/h. The drift can be further reduced by measures such as minimization of osmotic effects across the membrane, optimization of the parameters in closed-loop temperature control, and development of improved capacitance measurement circuitry. The low drift demonstrates that our device holds potential to offer highly stable measurements for long-term CGM.

VI. Conclusion

This paper has presented a MEMS affinity CGM sensor that uses capacitive transduction principles. The device consists of a Parylene diaphragm, which vibrates under magnetic excitation inside a microchamber and whose deflection is measured capacitively. The microchamber is filled with a solution of PAA-*ran*-PAAPBA and equipped with a cellulose acetate semipermeable membrane. PAA-*ran*-PAAPBA is a biocompatible polymer that specifically recognizes glucose by affinity binding; the semipermeable membrane prevents the polymer from escaping while allowing permeation of glucose into and out of the chamber. Affinity binding between the polymer and glucose results in the cross-linking of the polymer and an increase in the viscosity of the solution. Thus, by measuring the damped diaphragm vibration in the solution, the glucose concentration can be determined. The MEMS sensor vibration characteristics obtained at several selected glucose concentrations indicated that the device was capable of resolving glucose concentration changes by viscosity measurements. By fitting the experimental data to a simple 1-DOF mass-spring-damper model, the device's natural frequency was estimated to be 1190 Hz, while the dimensionless damping ratio increased from 0.37 to 0.44 as the glucose concentration varied from 30 to 360 mg/dL, reflecting the steady increase of the viscosity of the polymer solution with glucose concentration. Experimental results have also shown that the device responded quite rapidly to glucose concentration variations with time constants of approximately 1.5 min. This is shorter than the time responses of commercially available electrochemical CGM sensors and can be further reduced by improved MEMS design. In addition, it was also observed from the experimental data that the device response to glucose concentration changes was highly reversible. For example, as the glucose concentration was changed from 90 to 120 mg/dL and then reversed to 90 mg/dL, the deviation in the diaphragm vibration amplitude was only 60 ppm. Finally, we demonstrated that the device response was highly stable. For example, as the glucose concentration was held constant at 90 mg/dL,

Authorized licensed use limited to: Columbia University. Downloaded on January 19, 2010 at 13:06 from IEEE Xplore. Restrictions apply.

the drift rate in the diaphragm vibration amplitude was only 0.17 ppm/h. These results demonstrate that the MEMS sensor holds the potential to be used as a subcutaneously implanted device for long-term, stable, and reliable continuous monitoring of glucose in practical diabetes management.

REFERENCES

[1] MiniMed Paradigm REAL-Time Insulin Pump and Continuous Glucose Monitoring System, Medtronic MiniMed, Inc., San Antonio, TX, USA, 2006.

[2] FreeStyle Navigator Continuous Glucose Monitoring System, Abbott Diabetes Care, Inc., Alameda, CA, USA, 2008.

[3] DexCom Seven Plus System, Dexcom, Inc., San Diego, CA, USA, 2009.

[4] A. Heller, "Implanted electrochemical glucose sensors for the management of diabetes," *Annu. Rev. Biomed. Eng.*, vol. 1, pp. 153–175, 1999.

[5] J. S. Schultz, S. Mansouri, and I. J. Goldstein, "Affinity sensor—A new technique for developing implantable sensors for glucose and other metabolites," *Diabetes Care*, vol. 5, no. 3, pp. 245–253, May 1982.

[6] J. Schultz and G. Sims, "Affinity sensors for individual metabolites," *Biotechnol. Bioeng. Symp.*, vol. 9, pp. 65–71, 1979.

[7] Y. Zhao, S. Li, A. Davidson, B. Yang, Q. Wang, and Q. Lin, "A MEMS viscometric device for continuous glucose monitoring," *J. Micromech. Microeng.*, vol. 17, no. 12, pp. 2528–2537, Dec. 2007.

[8] U. Beyer, R. Ehwald, and L.-G. Fleischer, "Post-stress thickening of dextran/concanavalin A solutions used as sensitive fluids in a viscosimetric affinity assay for glucose," *Biotechnol. Prog.*, vol. 13, no. 6, pp. 722–726, 1997.

[9] T. Kataoka, F. Oh-Hashi, and Y. Sakurai, "Immunogenicity and amplifier cell production by tumor vaccines enhanced by concanavalin A," *Gann*, vol. 73, no. 2, pp. 193–205, Apr. 1982.

[10] H. Matsuura, S. Ranganathan, M. Yamamoto, and B. A. Kattke, "Studies on the effect of concanavalin A on the metabolism of low density lipoproteins in skin fibroblasts," *Jpn. J. Med.*, vol. 26, no. 3, pp. 323–325, Aug. 1987.

[11] K. Kataoka and A. Matsumoto, "Totally synthetic polymer gels responding to external glucose concentration: Their preparation and application to on-off regulation of insulin-release," *J. Amer. Chem. Soc.*, vol. 120, pp. 12 694–12 695, 1998.

[12] T. D. James, K. R. A. S. Sandanayake, and S. Shinkai, "Saccharide sensing with molecular receptors based on boronic acid," *Angew. Chem. Int. Ed. Engl.*, vol. 35, no. 17, pp. 1910–1922, Sep. 1996.

[13] J. Yan, H. Fang, and B. Wang, "Boronolectins and fluorescent boronolectins: An examination of the detailed chemistry issues important for the design," *Med. Res. Rev.*, vol. 25, no. 5, pp. 490–520, Sep. 2005.

[14] M. Lei, A. Baldi, E. Nuxoll, R. A. Siegel, and B. Ziaie, "A hydrogel-based implantable micromachined transponder for wireless glucose measurement," *Diabetes Technol. Ther.*, vol. 8, no. 1, pp. 112–122, Feb. 2006.

[15] F. H. Arnold, W. Zheng, and A. S. Michaels, "A membrane-moderated, conductimetric sensor for the detection and measurement of specific organic solutes in aqueous solutions," *J. Membr. Sci.*, vol. 167, no. 2, pp. 227–239, Mar. 2000.

[16] S. Li, X. Huang, E. N. Davis, Q. Lin, and Q. Wang, "Development of novel glucose sensing fluids with potential application to microelectromechanical systems-based continuous glucose monitoring," *J. Diabetes Sci. Technol.*, vol. 2, no. 6, pp. 1066–1074, Nov. 2008.

[17] S. Li, E. N. Davis, J. Anderson, Q. Lin, and Q. Wang, "Development of boronic acid grafted random copolymer sensing fluid for continuous glucose monitoring," *Biomacromolecules*, vol. 10, no. 1, pp. 113–118, Jan. 2009.

[18] X. X. Cai, A. Glidle, and J. M. Cooper, "Miniaturized electroanalytical sensor systems in micromachined structures," *Electroanalysis*, vol. 12, no. 9, pp. 631–639, May 2000.

[19] S. I. Park, S. B. Jun, S. Park, H. C. Kim, and S. J. Kim, "Application of a new Cl-plasma-treated Ag/AgCl reference electrode to micromachined glucose sensor," *IEEE Sensors J.*, vol. 3, no. 3, pp. 267–273, Jun. 2003.

[20] K. Chinami, Y. Akira, K. Keishin, H. Kohji, and M. Kunio, "Study on sensing system configuration by MEMS technology," *IEIC Tech. Rep.*, vol. 104, pp. 13–18, 2004.

[21] J. Wang, M. P. Chatrathi, B. M. Tian, and R. Polsky, "Microfabricated electrophoresis chips for simultaneous bioassays of glucose, uric acid, ascorbic acid, and acetaminophen," *Anal. Chem.*, vol. 72, no. 11, pp. 2514–2518, Jun. 2000.

[22] B. Xie, K. Ramanathan, and B. Danielsson, "Mini/micro thermal biosensors and other related devices for biochemical/clinical analysis and monitoring," *Trends Anal. Chem.*, vol. 19, no. 5, pp. 340–349, May 2000.

[23] P. Bataillard, "Calorimetric sensing in bioanalytical chemistry: Principles, applications and trends," *Trends Anal. Chem.*, vol. 12, no. 10, pp. 387–394, Nov./Dec. 1993.

[24] C. Pu, Z. Zhu, and Y.-H. Lo, "A surface-micromachined optical self-homodyne polarimetric sensor for noninvasive glucose monitoring," *IEEE Photon. Technol. Lett.*, vol. 12, no. 2, pp. 190–192, Feb. 2000.

[25] M. Paranjape, J. Garra, S. Brida, T. Schneider, R. White, and J. Currie, "A PDMS dermal patch for non-intrusive transdermal glucose sensing," *Sens. Actuators A, Phys.*, vol. 104, no. 3, pp. 195–204, May 2003.

[26] Y. Lin, D. W. Matson, D. E. Kurath, J. Wen, F. Xiang, W. D. Bennett, P. M. Martin, and R. D. Smith, "Microfluidic devices on polymer substrates for bioanalytical applications," in *Microreaction Technology: Industrial Prospects*, W. Ehrfeld, Ed. New York: Springer-Verlag, 2000, pp. 451–460.

[27] X. Huang, S. Li, J. S. Schultz, Q. Wang, and Q. Lin, "A MEMS affinity glucose sensor using a biocompatible glucose-responsive polymer," *Sens. Actuators B, Chem.*, vol. 140, no. 2, pp. 603–609, Jul. 2009.

[28] R. W. Baker, *Membrane Technology and Applications*., 2nd ed. Chichester, U.K.: Wiley, 2004.

Xian Huang received the B.S. and M.S. degrees in measurement and control technology and instrumentation from Tianjin University, Tianjin, China, in 2004 and 2007, respectively. He is currently working toward the Ph.D. degree in mechanical engineering at Columbia University, New York, NY.

His research interests are in the development of implantable miniature biosensors for diagnostic and therapeutic applications.

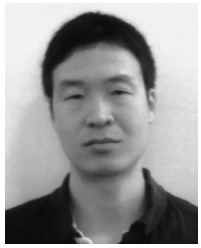

Siqi Li received the B.E. degree in polymer materials and engineering from Hefei University of Technology, Hefei, China, in 1998, the M.S. degree in polymer chemistry and physics from the University of Science and Technology of China, Hefei, in 2001, and the M.S. degree in organic chemistry from The University of Iowa, Iowa City, in 2004. He is currently working toward the Ph.D. degree in the Department of Chemistry and Biochemistry, University of South Carolina, Columbia.

His research interests are the development of glucose sensing polymer for continuous glucose monitoring, polymer and nanoparticle self-assembly, and nanoparticle bioconjugations for cancer therapy.

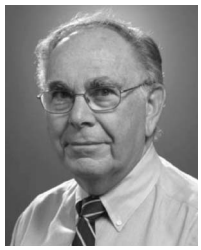

Jerome Schultz received the B.S. and M.S. degrees in chemical engineering from Columbia University, New York, NY, in 1954 and 1956, respectively, and the Ph.D. degree in biochemistry from the University of Wisconsin, Madison, in 1958.

He started his career as a Group Leader in the pharmaceutical industry (Lederle Laboratories) and then joined the University of Michigan, Ann Arbor, where he was the Chairman of the Department of Chemical Engineering. He spent two years at the National Science Foundation as the Deputy Director of the Engineering Centers Program. In 1987, he joined the University of Pittsburgh, Pittsburgh, PA, as the Director of the Center for Biotechnology and Bioengineering, where he was the Founding Chairman of the Department of Bioengineering. In 2003, he spent a year at NASA's Ames Research Center as a Senior Scientist in their Fundamental Biology Program. Since 2004, he has been a member of the faculty at the University of California, Riverside, as a Distinguished Professor and the Chairman of the Department of Bioengineering. His research interests include biosensors, membrane transport phenomena, transport processes in tissues, pharmacokinetics, and immobilized enzymes.

Dr. Schultz is a member of the National Academy of Engineering, a Fellow of the Biomedical Engineering Society, a Fellow of the American Association for the Advancement of Sciences, and a Founding Fellow and former President of the American Institute for Medical and Biological Engineering. He is an Editor of *Biotechnology Progress*.

Authorized licensed use limited to: Columbia University. Downloaded on January 19, 2010 at 13:06 from IEEE Xplore. Restrictions apply.

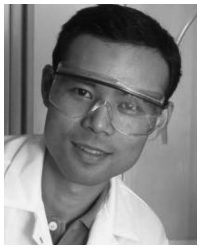

Qian Wang received the B.S. and Ph.D. degrees in chemistry from Tsinghua University, Beijing, China, in 1992 and 1997, respectively.

After postdoctoral research with Prof. M. Schlosser at the University of Lausanne, Lausanne, Switzerland, and with Prof. M. G. Finn at the Scripps Research Institute, he started as an Assistant Professor at the University of South Carolina, Columbia, in 2003, where he has been an Associate Professor since 2008 and the Robert L. Sumwalt Professor of Chemistry since 2009. His research interest focuses on the development of novel biomaterials and the understanding of cell behavior using self-assembled materials as a scaffold.

Qiao Lin received the Ph.D. degree in mechanical engineering from the California Institute of Technology, Pasadena, in 1998, with thesis research in robotics.

He conducted postdoctoral research in microelectromechanical systems (MEMS) at the Caltech Micromachining Laboratory from 1998 to 2000 and was an Assistant Professor of mechanical engineering at Carnegie Mellon University, Pittsburgh, PA, from 2000 to 2005. He has been an Associate Professor of mechanical engineering at Columbia University, New York, NY, since 2005. His research interests are in designing and creating integrated micro/nanosystems, particularly MEMS and microfluidic systems, for biomedical applications.

Authorized licensed use limited to: Columbia University. Downloaded on January 19, 2010 at 13:06 from IEEE Xplore. Restrictions apply.